Archival Report

Biological Psychiatry: Celebrating 50 Years

Heroin Cue–Evoked Astrocytic Structural Plasticity at Nucleus Accumbens Synapses Inhibits Heroin Seeking

Anna Kruyer, Michael D. Scofield, Daniel Wood, Kathryn J. Reissner, and Peter W. Kalivas

ABSTRACT

BACKGROUND: Opioid addiction is a critical medical and societal problem characterized by vulnerability to relapse. Glutamatergic synapses in the nucleus accumbens regulate the motivation to relapse to opioid use, and down-regulation of glutamate transporters on astroglial processes adjacent to accumbens synapses contributes to heroin seeking induced by cues. However, it is not known how astroglial processes themselves respond to heroin cues or if changes in astroglial morphology are necessary for heroin seeking.

METHODS: Male Sprague Dawley rats (n = 62) were trained to self-administer heroin or sucrose and were reinstated by heroin-conditioned or sucrose-conditioned cues. Astroglial proximity to accumbens synapses was estimated using a confocal-based strategy, and the association between digitally isolated astroglia and the presynaptic marker synapsin I was quantified. To determine the functional consequence of astroglial morphological plasticity on cued heroin seeking, a morpholino antisense strategy was used to knock down expression of the actin binding protein ezrin, which is expressed almost exclusively in peripheral astroglial processes in the adult rat brain.

RESULTS: After heroin extinction, there was an enduring reduction in synaptic proximity by astroglia. Synaptic proximity was restored during 15 minutes of cued heroin seeking but returned to extinction levels by 120 minutes. Extinction from sucrose self-administration and reinstated sucrose seeking induced no changes in astroglial synaptic association. Ezrin knockdown reduced astroglial association with synapses and potentiated cued heroin seeking.

CONCLUSIONS: Cue-induced heroin seeking transiently increased synaptic proximity of accumbens astrocytes. Surprisingly, the reassociation of astroglia with synapses was compensatory, and preventing cue-induced morphological plasticity in astrocytes potentiated heroin seeking.

Keywords: Addiction, Astrocyte, Heroin, Nucleus accumbens, Self-administration, Synapse

https://doi.org/10.1016/j.biopsych.2019.06.026

Astrocytes are the most abundant glial cell type in the brain. They have long been considered support cells for maintaining neuronal metabolic homeostasis, and a growing literature demonstrates that astrocytes directly regulate neuronal activity, in part through peripheral processes that contact up to 90% of synapses in some brain regions (1,2). The peripheral processes of astrocytes are irregular protrusions lacking glial fibrillary acidic protein (GFAP)–containing filaments, microtubules, and organelles (3) that in vitro undergo structural plasticity in response to excitatory synaptic activity (4). Astrocytes also regulate levels of extracellular glutamate via uptake and release and promote the stability of dendritic spines (5). Their capacity to simultaneously interact with tens of thousands of synapses physically situates astrocytes to coordinate neurocircuit dynamics and play a role in circuit pathologies thought to underlie neuropsychiatric disorders (6).

Astrocytes gather information from neurons via the spillover of synaptically released transmitters, and spillover of glutamate in the core subcompartment of the nucleus accumbens (NAcore) is necessary for drug-associated, but not sucrose-associated, cues to reinstate seeking in rodent models of cue-induced relapse (7,8). Although the shell subcompartment of the NA is also involved in the processing of drug-reward contingencies and contributes to drug seeking in response to drug-associated contexts and priming injections, we focus here on the NAcore because of its central role in producing seeking behavior in response to drug-associated cues (8). Glutamate spillover in the NAcore arises because repeated administration of all addictive drugs examined to date, including cocaine, heroin, nicotine, and alcohol, reduces the expression and/or function of the glial glutamate transporter (GLT-1) (7,8), which is preferentially expressed on astroglial processes (9,10). Moreover, computational modeling of astroglial perisynaptic processes demonstrates that astroglial insulation along 50% of the synaptic perimeter doubles glutamate concentrations within the synaptic cleft and produces a 2- to 4-fold decrease in extrasynaptic glutamate (11). Thus, through morphological plasticity, astrocyte cytoarchitecture regulates the balance between

ISSN: 0006-3223

synaptic and extrasynaptic glutamate (12). Although drug-induced reductions in NAcore GLT-1 are linked to relapse in animal models of addiction, the capacity of the astroglial membrane to undergo rapid morphological changes in vitro indicates that changes in astrocyte morphology and synaptic proximity may also impact extracellular glutamate levels in vivo and regulate the capacity of drug cues to initiate seeking. In this study, we demonstrate that the in vivo association of astrocytes with the presynaptic marker synapsin I (13) in the NAcore is constitutively reduced after heroin use and is transiently restored by cues that predict heroin delivery. To determine the functional consequence of the morphological plasticity we observed in NAcore astrocytes in response to heroin cues, we took advantage of the fact that ezrin is an actin-binding protein expressed primarily by astrocytes in the adult rat brain that links actin with the astroglial membrane in peripheral processes (14,15). We show that knockdown of ezrin reduced astroglial association with the synapse and elevated cued heroin seeking, suggesting an important role for transient astroglial plasticity in attenuation of drug seeking.

METHODS AND MATERIALS

Self-administration

Male Sprague Dawley rats (200–250 g) were purchased from Charles River Laboratories (Wilmington, MA) and housed individually in a temperature-controlled environment on a 12-hour reverse light/dark cycle. Following approximately 1 week of acclimation, animals undergoing heroin self-administration or receiving yoked saline infusions were anesthetized with ketamine/xylazine (100 mg/kg and 7 mg/kg, intramuscularly) and fitted with intrajugular catheters. Ketorolac (2 mg/kg, intraperitoneally) was administered postoperatively as an analgesic, and taurolidine-citrate catheter lock solution (0.05 mL) (Access Technologies, Skokie, IL) was administered intravenously through the catheter beginning 48 hours after surgery and daily thereafter to maintain patency. Heroin or sucrose self-administering rats and yoked control rats were maintained on 25 g chow/day during the self-administration phase of operant training and received chow ad libitum thereafter. Animals were trained to self-administer sucrose (orally) or heroin (intravenously) during 3-hour sessions for 10 consecutive days, during which time presses on an active lever were paired with light and tone cues and either infusion of heroin (100 μg/infusion on days 1 and 2, 50 μg/infusion on days 3 and 4, 25 μg/infusion on all subsequent days) or delivery of a sucrose pellet (45 mg) (Bio-Serv, Flemington, NJ).

The dosing strategy during heroin self-administration ensures that animals acquire self-administration and lever discrimination early during operant training (days 1–2) and serves to elevate lever pressing above baseline after acquisition of operant responding (days 5–10). Yoked control animals received light and tone cues when a paired rat received sucrose or heroin. Animals yoked to heroin self-administering rats also received passive infusions of saline. Following self-administration, animals underwent 10–14 days of extinction training (3 hours/day) during which time presses on the active lever had no consequence. Extinguished animals and yoked control animals were sacrificed 24 hours after the last extinction session. Reinstated animals were placed in the operant chamber a final time, and light and tone pairings were restored to the active lever, but animals received no reward. The session continued for 15 minutes or 120 minutes before sacrifice. Animals with >10 active lever presses within the first 15 minutes of reinstatement trials were considered to reinstate and were included in subsequent analyses. All animals were anesthetized with pentobarbital (20 mg, intravenously) and perfused transcardially with 60 mL 0.1-mol/L phosphate buffer and 120 mL 4% paraformaldehyde. Brains were removed, incubated overnight in 4% paraformaldehyde, and sliced at 100 μm on a vibrating-blade microtome (Thermo Fisher Scientific, Waltham, MA). Tissue was collected into phosphate-buffered saline (PBS) with 0.05% sodium azide and stored at 4°C until use.

Viral Labeling and Immunohistochemistry

Immediately following catheter implantation or 5 days before the start of sucrose self-administration, animals received microinjections (1.0 μL/hemisphere, 0.15 μL/min, 5-minute diffusion) of a virus driving expression of membrane-targeted mCherry under control of the GFAP promoter (adeno-associated virus 5-GFAP-hM3dq-mCherry; University of Zurich, Zurich, Switzerland). mCherry was tagged to hM3dq, which is a membrane-targeted Gq-coupled DREADD (designer receptor exclusively activated by designer drug). For the experiments in this report, DREADD was used only for membrane targeting of mCherry and was not activated. The virus was injected into the NAcore (+1.5 mm anteroposterior, ±1.8 mm mediolateral, −7.0 mm dorsoventral) with 26-gauge injectors (Plastics One Inc., Roanoke, VA). Virus incubation occurred during recovery from surgery and over the course of self-administration and extinction training (approximately 4 weeks). Following perfusion and sectioning, slices containing the NAcore were permeabilized in 1× PBS with 2% Triton X-100 for 1 hour at room temperature before blocking in 1× PBS with 0.2% Triton X-100 (PBST) with 2% normal goat serum (block). Primary antibodies against synapsin I (1:1000; Abcam, Cambridge, UK), ezrin (1:1000; Cell Signaling Technology, Danvers, MA), radixin (Abcam), moesin (Abcam), or phospho-ezrin (Thr567)/radixin (Thr564)/moesin (Thr558) (1:1000; Cell Signaling Technology) were diluted in block, and sections were incubated for 2 days at 4°C with gentle agitation. Virally expressed mCherry was visualized without antibody amplification. Slices were washed in PBST before incubation in fluorescent secondary antibodies (Alexa Fluor, 1:1000; Thermo Fisher Scientific) in PBST for 1 day at room temperature. After washing in PBST, tissue was mounted onto glass slides and covered with a coverslip using ProLong Gold Antifade Mountant (Thermo Fisher Scientific).

Imaging Acquisition and Analysis

Z-stacks were acquired using a Leica SP5 laser scanning confocal microscope (Leica Microsystems Inc., Wetzlar, Germany) equipped with argon, krypton and helium/neon beams. All images were acquired using a 63× oil immersion objective lens with 1.7× digital zoom, 1024 × 1024 frame size, 12-bit image resolution, 4-frame averaging, and 1-μm step size. Astrocytes were acquired if and only if the entire cellular volume could be imaged within the tissue section and the boundaries

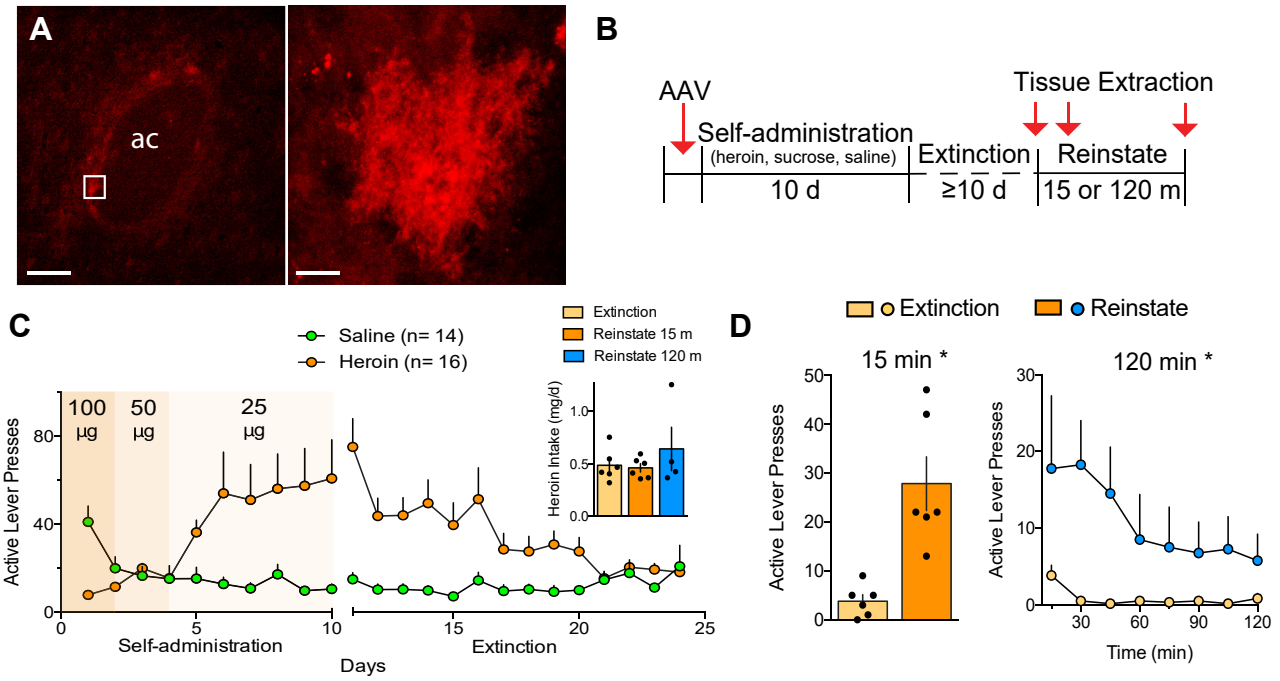

Figure 1. Heroin self-administration and cue-induced heroin seeking. **(A)** Representative transfection of astroglia in the nucleus accumbens core with an adeno-associated virus (AAV) driving membrane-bound mCherry under the glial fibrillary acidic protein promoter. Low magnification (left panel) shows multiple filled astroglia adjacent to the anterior commissure (ac) (scale bar = 150 μm), and high magnification (right panel) shows a single astrocyte (scale bar = 10 μm). **(B)** Outline of the protocol used throughout the article. **(C)** Active lever pressing during heroin self-administration and extinction training (see Supplemental Figure S2 for inactive lever pressing). Inset shows that the treatment groups infused the same total amount of heroin (1-way analysis of variance, $F_{2,13}$ = 0.84, p = .455). **(D)** Cue-induced reinstatement for 15 minutes or 120 minutes elevated active lever pressing compared with the first 15 minutes of the final extinction trial (15 minutes, paired Student t_5 = 3.77, *p = .013; 120 minutes, 2-way repeated measures analysis of variance, $F_{1,3}$ = 10.06, *p = .050). Data shown as mean ± SEM.

of the cell were not overlapping with nearby labeled cells. Acquired stacks were iteratively deconvolved 10 times (AutoQuant; Media Cybernetics, Rockville, MD). Digital analysis of mCherry signal intensity relative to proximal background intensity was used to build a digital model of the astroglial volume (Bitplane Imaris; Oxford Instruments, Abingdon, UK). Colocalization (astrocyte with synapsin I, astrocyte with ezrin, astrocyte surface with phosphorylated-ezrin/radixin/moesin [p-ERM]) was determined based on thresholded signal intensity in each channel. Voxels containing fluorescence signal intensity greater than noise for each channel, determined empirically using a two-dimensional scatter plot within the colocalization module, were used to build a colocalization channel and acquire volume, puncta number, and puncta volume parameters. Total synapsin I, radixin, and moesin immunoreactivity was determined based on thresholded signal intensity and normalized to the volume of the frame from which it was acquired. Surface expression was determined by excluding colocalized signal >200 nm from the astrocyte membrane. All imaging and image analyses were conducted blinded to animal treatment.

Ezrin Knockdown

Animals undergoing treatment with antisense or control Vivo-Morpholino (Gene Tools, LLC, Philomath, OR) received bilateral cannulae placed just above the NAcore immediately following catheter surgery. Guide cannulae were used for viral labeling before operant training and for application of ezrin antisense or control oligomers during extinction training. Beginning on day 7 of extinction for 3 consecutive days, animals received bilateral infusions (1 μL, 0.15 μL/min, 5-minute diffusion) of an antisense oligomer targeted to ezrin (GCGCTCCGCAGGTTTCACTTCGTGA, 50 μmol/L) or a nonspecific control sequence (Gene Tools, LLC, Philomath, OR). After 3 additional days of extinction training, animals were reinstated using cues, and their behavior was monitored.

Experimental Design and Statistical Analysis

All numerical data were analyzed using GraphPad Prism 7 (GraphPad Software, San Diego, CA) and are presented as scatter plots with the median indicated for each group. For each measure, data were analyzed using D'Agostino-Pearson omnibus normality test followed by Kruskal-Wallis nonparametric test, because in all cases at least one treatment group was found to be not normally distributed (Supplemental Table S1). Additionally, cumulative distribution plots of yoked saline measurements were used to identify 3 equal subpopulations of astroglia for each measure. Population criteria were applied across all treatment groups, and differences between treatment groups in astroglial subpopulations were

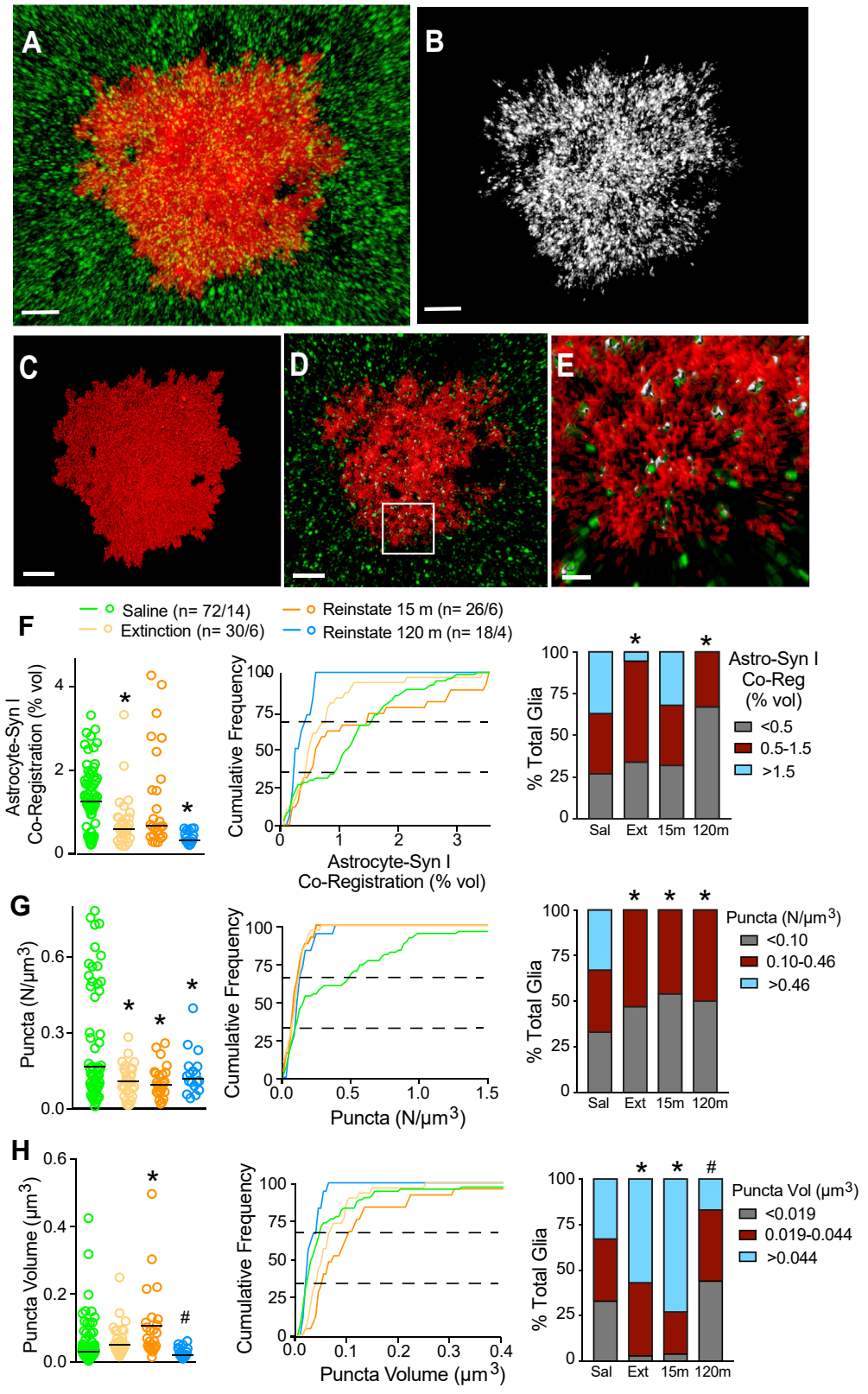
A
B
C
D
E
F
Saline (n= 72/14)
Extinction (n= 30/6)
Reinstate 15 m (n= 26/6)
Reinstate 120 m (n= 18/4)
Astrocyte-Syn I Co-Registration (% vol)
Cumulative Frequency
Astrocyte-Syn I Co-Registration (% vol)
% Total Glia
Astro-Syn I Co-Reg (% vol)
<0.5
0.5-1.5
>1.5
Sal
Ext
15m
120m
G
Puncta (N/μm3)
Cumulative Frequency
Puncta (N/μm3)
% Total Glia
Puncta (N/μm3)
<0.10
0.10-0.46
>0.46
H
Puncta Volume (μm3)
Cumulative Frequency
Puncta Volume (μm3)
% Total Glia
Puncta Vol (μm3)
<0.019
0.019-0.044
>0.044

determined using χ^2 test. In all cases, p values $< .05$ were considered significant.

RESULTS

Heroin and Sucrose Self-administration, Extinction, and Cued Seeking

Before beginning heroin self-administration, NAcore astroglia were transfected with a membrane reporter (adeno-associated virus 5-GFAP-hM3dq-mCherry) to allow confocal imaging, digitization, and quantification of cell morphology (Figure 1A). As all animals in this study received virus infusions and all imaged astrocytes expressed the membrane tag, any potential alterations in calcium flux or G protein–coupled receptor signaling induced by the DREADD would be expected to be equivalent across groups. Rats were trained to self-administer heroin or were yoked saline control animals (Figure 1B, C; Supplemental Figure S1 for inactive lever presses). The heroin-trained rats were divided into 3 treatment groups such that all groups had the same total heroin intake (Figure 1C, inset). Lever pressing was extinguished over 10 to 14 days of training where heroin and cues were not delivered in response to active lever presses (Figure 1B, C). Heroin seeking was then induced in the absence of heroin delivery by restoring the light and tone cues previously associated with heroin infusion, and NAcore tissue slices were obtained 15 minutes or 120 minutes after initiating cued heroin seeking (Figure 1B). Heroin cues reinstated active lever pressing relative to extinction levels of pressing after either 15 minutes or 120 minutes, and the peak response occurred during the first 45 minutes of drug seeking (Figure 1D). A separate group of rats was trained to self-administer sucrose pellets using the same extinction and cue-induced reinstatement protocol as for heroin (Supplemental Figure S2). Extinguished and reinstated rats were matched for average daily sucrose delivery (Supplemental Figure S2A, inset), and rats reinstated to a similar level relative to cued heroin seeking in response to sucrose-paired cues (Supplemental Figure S2B).

Astrocyte Labeling and Morphology

Astrocytes in the NAcore that were fully transfected with the mCherry membrane reporter were imaged and rendered using Imaris software (Figure 2 and Supplemental Figure S3). The digitally isolated and rendered astrocytes revealed a highly convoluted and irregular membrane surface, a morphological characteristic easily seen in a single z-plane obtained near the center of the cell (Figure 2D, E; Supplemental Figure S3). Astroglia are estimated to contact 20,000 to 160,000 individual synapses (16), but it is unknown to what extent astroglial interactions with synapses undergo plasticity in the adult brain. To estimate synaptic proximity by astroglia, tissue was double-labeled for the presynaptic marker synapsin I (Figure 2A). Coregistration of immunoreactive synapsin I puncta with the astroglial surface was digitally isolated and quantified to estimate the near-adjacency of astroglial membrane with NAcore synapsin I (Figure 2B). This approach was developed because the diameter of fine astroglial processes [50–200 nm (17)] is below the limit of resolution for confocal microscopy [approximately 250 nm (18)]. In the striatum, the distance of peripheral astroglial processes from excitatory synapses ranges from 10 to 400 nm, with 53% of synapses having astroglial coverage at a distance of <10 nm (19). Thus, in the present report, we operationally define near-adjacency as synapsin I puncta coregistered with the astroglial membrane reporter by being within the 250-nm limit of image resolution (Figure 2E).

Examining a single plane from the z-stack near the middle of the astroglial volume showed that the astroglial surface extended throughout the astrocyte, and the presence of coregistered synapsin I revealed abundant points of contact near the geometric center of the cell volume (Figure 2E, Supplemental Figure S3). Total synapsin I labeling between treatment groups was not different (Supplemental Figure S4A), indicating that the changes in the heroin-trained rats arose from alterations in astroglial morphology, not synapsin I density.

Heroin-Associated Cues Restore Synaptic Proximity of NAcore Astrocytes

Coregistration of the astroglial membrane with synapsin I in the NAcore was reduced after extinction from heroin compared with yoked saline rats (Figure 2F), akin to our previous report in rats extinguished from cocaine self-administration (20). However, after 15 minutes of cue-induced heroin seeking, we observed rapid, transient reassociation of astrocytic processes with synapsin I that returned to extinction levels by 120 minutes after initiating cued reinstatement (Figure 2F, left panel).

In accord with previous reports (6,20), astroglial volume ranged from 5000 to 50,000 μm^3 across all experimental groups (Supplemental Figure S5). Because astroglial volume

Figure 2. Coregistration of the astroglial membrane with synapsin I undergoes transient plasticity during cued heroin seeking. **(A)** Representative confocal image of an astrocyte (red) that was counterstained for immunoreactive synapsin I (green). **(B)** Digitally isolated synapsin I puncta that coregistered with the astroglial membrane (within 250 nm). **(C)** Digital rendering of astrocyte in panel **(A)**. **(D)** A single plane from the middle of the z-axis in panel **(A)**. **(E)** Coregistered astroglial membrane (red) and synapsin I (green) from the box in panel **(D)**. Astroglial membrane within 250 nm of synapsin I puncta is colored white; synapsin I puncta not within the 250-nm limit of resolution are colored green. **(F)** Synaptic proximity of the astroglial membrane was constitutively reduced after extinguished withdrawal and transiently increased during 15 minutes of cued heroin seeking (left panel shows raw data, Kruskal-Wallis = 18.8, $p < .001$; middle panel shows cumulative frequency plots; right panel shows subpopulations: $\chi^2_6 = 23.78$, $p < .001$). **(G)** The number of coregistered puncta was reduced after heroin self-administration (left panel shows raw data, Kruskal-Wallis = 16.42, $p = .001$; middle panel shows frequency plots; right panel shows subpopulations: $\chi^2_6 = 29.86$, $p < .001$). **(H)** Average volume of colocalized puncta was increased after 15 minutes of reinstated heroin seeking (left panel shows raw data, Kruskal-Wallis = 25.8, $p < .001$; middle panel shows frequency plots; right panel shows subpopulations: $\chi^2_6 = 27.51$, $p < .001$). $^*p < .05$, compared with saline using a Dunn post hoc test (left panel) or multiple χ^2 tests with a Bonferroni adjustment for multiple comparisons (right panel); $^\#p < .05$, compared with 15 minutes of reinstatement. **(A–D)** Scale bar = 10 μm. **(E)** Scale bar = 2 μm. **(F–H)** Left panel, scale bar = median. Astro, astrocyte; Co-Reg, coregistration; Syn I, synapsin I; Vol, volume.

was reduced in rats reinstated for 15 minutes, data were analyzed with (Figure 2F) and without (Supplemental Figure S4B) normalizing synaptic coverage to total astroglial volume. In both comparisons, the 15-minute reinstated group showed increased astroglia–synapsin I proximity compared with extinguished rats.

Values for astroglia–synapsin I proximity were not normally distributed in control rats (Supplemental Table S1). Accordingly, we more closely examined the distribution of astroglia-synaptic proximity using cumulative frequency plots (Figure 2F–H, middle panel) that showed differences between treatment groups, and nonlinear breaks in the distribution curves supported possible subpopulations. Thus, data were divided into 3 subpopulations according to the values producing 3 equal populations in control rats (Figure 2F–H, right; i.e., top, middle and bottom thirds). A χ^2 analysis revealed that compared with saline rats, the extinguished group had nearly complete elimination of the astroglial subgroup containing the most astroglia–synapsin I coregistration (Figure 2F, right). However, this subclass transiently returned after 15 minutes of cued reinstatement. In contrast to heroin-trained rats, rats extinguished from sucrose self-administration or reinstated to sucrose-associated cues showed no alterations in astroglia–synapsin I proximity (Supplemental Figure S4C).

Cued Astroglia–Synapsin I Coregistration Results From Larger Regions of Overlap, Not Increased Number of Contacts

We next examined whether the transient plasticity in astroglia–synapsin I proximity occurred because there were more synapsin I puncta in contact with the astroglial membrane or the volume of overlapping regions had increased. Surprisingly, the number of puncta indicating near-adjacency between the astroglial membrane and synapsin I did not change during 15 minutes of reinstated seeking (Figure 2G). Accordingly, the subgroup of astroglia that demonstrated the highest number of near-adjacent regions was eliminated in all heroin-extinguished rats regardless of whether they underwent cued reinstatement (Figure 2G, right). In contrast, the volume of astroglia–synapsin I puncta showed dynamic changes after extinction and reinstatement (Figure 2H). Thus, the increased astroglia–synapsin I proximity after 15 minutes of cued reinstatement observed in Figure 2F arose from larger, but not more coregistered, puncta after 15 minutes of cued reinstatement and may indicate an increase in proximity on existing contacts (those $<$250 nm), rather than an increase in discrete points of contact between the astroglial membrane and synapsin I.

Ezrin Knockdown Inhibits Astroglia–Synapsin I Reassociation and Augments Cued Seeking

To examine the molecular underpinnings and functional relevance of the cue-induced astroglial morphological plasticity we observed, we examined the ERM family member protein ezrin and p-ERM. Ezrin and the other ERM proteins link the actin cytoskeleton with the astroglial membrane, allowing membrane protrusion and motility (21). In contrast with more widely distributed radixin and moesin, immunoelectron microscopy studies show that ezrin is highly selective for peripheral astroglial processes in the adult rat brain (14), with some evidence for expression in ependymal cells (22,23). Ezrin is also expressed in microglia and neurons during early postnatal development (24). When phosphorylated, ezrin and other ERM proteins link actin to the membrane of astroglial processes, thereby enabling membrane protrusion (25). Immunohistochemical analysis for p-ERM and nonphosphorylated ezrin showed reduced p-ERM in heroin-extinguished rats and restoration to control levels during 15 minutes of cued heroin reinstatement (Figure 3B). Importantly, total ezrin expression was equivalent across all treatment groups (Supplemental Figure S7). The changes in ERM phosphorylation after extinction and 15 minutes of reinstatement were consistent with the observed changes in astroglia–synapsin I association (Figure 2).

As ezrin exhibits the greatest selectivity for astroglial processes relative to radixin, moesin, or other actin binding proteins (14), we examined ezrin knockdown as a strategy to impair the synaptic reassociation by astrocytes during 15 minutes of cue exposure. Thus, another set of rats were trained to self-administer heroin and on day 7 of extinction training received bilateral infusions of an ezrin-targeted antisense oligomer in the NAcore for 3 consecutive days followed by 3 additional days of extinction training (Figure 3F). This timeline was selected because previous work demonstrates reduced protein expression 4 days following the last of 3 consecutive days of morpholino infusion (26). Animals receiving ezrin and control sequences exhibited no differences in overall heroin intake during self-administration or active lever pressing during the last 2 days of extinction training (Supplemental Figure S8A, B). Compared with a standard control oligomer, ezrin antisense markedly reduced ezrin protein detected by immunohistochemistry (Figure 3C, D) but did not alter radixin or moesin levels (Supplemental Figure S9). The ezrin-targeted morpholino also reduced astroglia–synapsin I association compared with control treatment by approximately the same percentage as extinction training (compare Figure 2F with Figure 3E). Therefore, ezrin knockdown by morpholino was used to impair the astrocyte-synapse reassociation induced by heroin cue exposure. When reinstated using heroin-associated cues, rats sustaining NAcore ezrin knockdown demonstrated greater active lever presses compared with control animals (Figure 3G), indicating a compensatory effect of the cue-induced astroglia–synapsin I reassociation. There was no alteration by ezrin knockdown on inactive lever presses (Supplemental Figure S8C).

DISCUSSION

We used a confocal-based strategy to demonstrate that rats extinguished from heroin self-administration have reduced astroglial proximity to the synaptic marker synapsin I in the NAcore. Although our work does not address the necessity of extinction training for this process, withdrawal appears necessary for retraction of astroglial processes from the synapse, as retraction was not observed 24 hours after discontinuing cocaine self-administration (27). Surprisingly, the constitutive reduction in synaptic proximity was reversed after

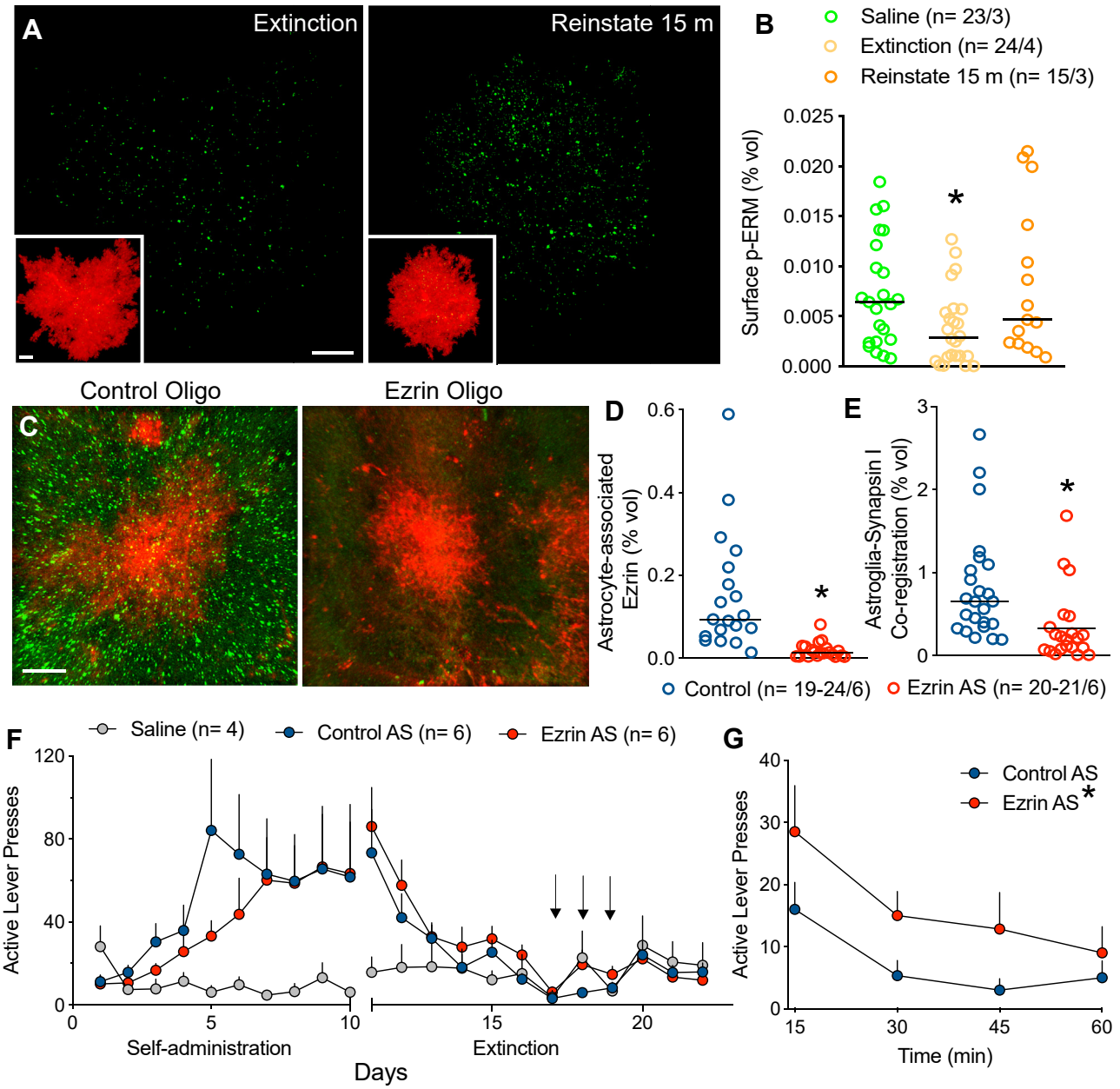

Figure 3. Ezrin knockdown prevents transient astroglial plasticity and promotes cue-induced heroin seeking. **(A, B)** Phosphorylated-ezrin/radixin/moesin (p-ERM) immunoreactivity was examined in tissue extracted from animals following extinction or after 15 minutes of reinstatement with heroin cues (see Supplemental Figure S6 for inset magnification). **(B)** Heroin cues elicited a significant elevation in p-ERM levels compared with levels observed in extinguished animals (Kruskal-Wallis = 7.483, *p = .0237), and an ezrin-targeted antisense oligomer was developed to knock down ezrin expression **(C, D)**. Relative to a control oligomer **(C)**, the ezrin-targeted morpholino oligomer produced 86% ezrin knockdown (reduction in green fluorescence) near the injection tract **(D)** (Mann-Whitney U test, *p = .0007). The ezrin-targeted oligomer also produced a profound reduction in synaptic association of astroglial membrane **(E)** (Mann-Whitney U test, *p = .0003). **(F)** Next, rats were trained to self-administer heroin for 10 days before undergoing extinction training. On day 7 of extinction, rats received bilateral infusions of the ezrin-targeted antisense oligomer or a control oligomer for 3 consecutive days in the nucleus accumbens core (arrows). Animals from both groups were reinstated using cues, and animals that underwent ezrin knockdown exhibited enhanced and prolonged reinstatement behavior compared with control animals **(G)** (two-way analysis of variance, $F_{1,40}$ = 8.193, *p = .0067, effect of treatment). In panels **(B, D, E)**, n is shown in legends as cells/animals. In panels **(F, G)**, data are shown as mean ± SEM; in panels **(B, D, E)**, data are shown as median. **(A)** Scale bar = 10 μm, scale bar (inset) = 10 μm (inset). **(C)** Scale bar = 20 μm. AS, antisense oligomer; Oligo, oligomer.

15 minutes of cued heroin seeking. This reversal was transient and returned to extinction levels by the end of the 120-minute reinstatement session, when active lever pressing had returned to the extinction baseline. The constitutive and cued transient changes in astroglia–synapsin I proximity were not recapitulated in the NAcore of rats extinguished from sucrose

self-administration and reinstated for 15 minutes using sucrose-associated cues. These data reveal remarkable rapid and transient astroglial morphological plasticity in response to cues that signal heroin availability and support the emerging conceptualization that astrocytes partner with canonical presynaptic and postsynaptic elements to regulate synaptic transmission and homeostasis (28–31). Importantly, the lack of astroglial plasticity in response to cues signaling sucrose availability indicate that the observed astroglial plasticity may be a process that countermands the excessive motivation to relapse experienced by opioid users.

Astroglial Plasticity Is Both Pathogenic and Compensatory

Synaptic spillover of glutamate during drug seeking is well documented using in vivo microdialysis or glutamate biosensors (8) as well as in vitro by measuring the effect of electrically stimulated glutamate release on the time constant of *N*-methyl-D-aspartate current decay (32). Spillover is thought to result from the fact that repeated treatment with most addictive drugs, including opioids, downregulates the astroglial glutamate transporter GLT-1. However, the constitutive reduction in astroglial proximity to synapsin I after cocaine (20) and heroin self-administration may also contribute to the capacity of drug cues to promote synaptic spillover in the NAcore. For example, the decreased astroglia-synapse proximity associated with heroin extinction would be expected to reduce the diffusion barrier through decreased synaptic insulation (11,33) and proximity of the already reduced levels of GLT-1 on processes near glutamatergic synapses (34). Indeed, the lack of glutamate spillover during cue-induced reinstatement of sucrose seeking likely arises because repeated sucrose use does not downregulate GLT-1 (8) or produce changes in astroglia–synapsin I proximity (Supplemental Figure S4C).

In contrast to the constitutive reduction in astroglia–synapsin I proximity after heroin withdrawal, the cue-induced restoration of proximity appeared to be compensatory. Thus, heroin cue–induced transient increases in synaptic proximity by astrocytes may compartmentalize glutamate spillover presynaptically, promoting the activation of release-regulating presynaptic glutamate autoreceptors and reducing the intensity and duration of cued reinstatement (35,36). This possibility is directly supported by our finding that downregulating ezrin to prevent the cued restoration of astroglia–synapsin I proximity facilitates cue-induced heroin seeking. The regulation of synaptic glutamate release and spillover by astroglial processes is consistent with the fact that a 3-fold to 4-fold increase in selective postsynaptic astroglial coverage produces a 2-fold to 4-fold increase in the likelihood that glutamate escaping the synapse will activate presynaptic release-inhibiting autoreceptors (11,37). Also, consistent with the idea that astroglial peripheral processes may provide a directional diffusion barrier, electron microscopy reveals that astroglial processes only partly contact synapses, with just 43% of the synaptic interface being contacted by astroglial membrane in rat hippocampus (38,39), Thus, cue-induced restoration of astroglial surfaces near the synapse could target synaptic glutamate spillover toward presynaptic metabotropic glutamate autoreceptors and thereby reduce cue-induced glutamate release and reinstated heroin seeking. Indeed, preventing transient increase in astroglia-synapse proximity by ezrin knockdown prolonged the duration of reinstated heroin seeking, indicating that the plasticity may directly contribute to the gradual decrease (within-trial extinction) in unrewarded lever pressing that occurs over the 2-hour reinstatement session.

Conclusions and Future Directions

Our data show that rat NAcore astrocytes undergo transient reassociation of astroglia-synapse proximity in response to heroin-associated cues and that this plasticity negatively regulates cue-induced heroin seeking. A compensatory role for transient astroglial plasticity contrasts the transient postsynaptic potentiation produced in NAcore medium spiny neurons (MSNs) during cue-induced drug seeking (40,41). The NAcore contains two subtypes of projection MSNs that selectively express either dopamine D_1 or D_2 receptors (42). Cued drug seeking is promoted by activating D1-MSNs or inhibiting D2-MSNs (43,44), and transient postsynaptic potentiation induced by drug cues occurs largely at D1-MSNs (45). Interestingly, individual astroglial calcium flux selectively occurs in response to activity of either D1-MSNs or D2-MSNs (46). The cell-specific associations by individual astroglia may contribute to the apparent subpopulations we observed in morphological characteristics, and it is interesting to speculate that the changes in astroglia–synapsin I proximity may occur selectively around D1-MSNs that harbor cue-induced transient postsynaptic potentiation. The apparently opposing actions of cue-induced astroglial and postsynaptic plasticity highlight the importance of considering all 4 synaptic compartments [presynapse, postsynapse, astroglial processes, and extracellular matrix (7,31)] to understand how synapses are homeostatically balanced in contributing to behavior. Moreover, understanding tetrapartite synaptic homeostasis may be an important prerequisite toward developing interventions for behavioral pathologies such as drug relapse.

ACKNOWLEDGMENTS AND DISCLOSURES

This work was supported by the National Institutes of Health (Grant Nos. DA007288 and DA044782 [to AK], Grant No. DA40004 [to MDS], Grant No. DA041455 [to KJR], and Grant Nos. DA003906 and DA012513) and the National Science Foundation (Grant No. OIA 1539034 [to PWK]).

We thank Kelsey Vollmer and Kyle Simpson for assistance with behavioral experiments.

The authors report no biomedical financial interests or potential conflicts of interest.

ARTICLE INFORMATION

From the Departments of Neurosciences (AK, MDS, DW, PWK) and Anesthesia and Perioperative Medicine (MDS), Medical University of South Carolina, Charleston, South Carolina; and Department of Psychology and Neuroscience (KJR), University of North Carolina at Chapel Hill, Chapel Hill, North Carolina.

Address correspondence to Anna Kruyer, Ph.D., or Peter W. Kalivas, Ph.D., 173 Ashley Avenue, MSC510, Charleston, SC, 29425; E-mail: kruyer@musc.edu (AK) or kalivasp@musc.edu (PWK).

Received Apr 3, 2019; revised Jun 6, 2019; accepted Jun 19, 2019.

Supplementary material cited in this article is available online at https://doi.org/10.1016/j.biopsych.2019.06.026.

REFERENCES

1. Zhang Q, Pangrsic T, Kreft M, Krzan M, Li N, Sul JY, *et al.* (2004): Fusion-related release of glutamate from astrocytes. J Biol Chem 279:12724–12733.
2. Bernardinelli Y, Muller D, Nikonenko I (2014): Astrocyte-synapse structural plasticity. Neural Plast 2014:232105.
3. Khakh BS, Sofroniew MV (2015): Diversity of astrocyte functions and phenotypes in neural circuits. Nat Neurosci 18:942–952.
4. Perez-Alvarez A, Navarrete M, Covelo A, Martin ED, Araque A (2014): Structural and functional plasticity of astrocyte processes and dendritic spine interactions. J Neurosci 34:12738–12744.
5. Bernardinelli Y, Randall J, Janett E, Nikonenko I, Konig S, Jones EV, *et al.* (2014): Activity-dependent structural plasticity of perisynaptic astrocytic domains promotes excitatory synapse stability. Curr Biol 24:1679–1688.
6. Halassa MM, Fellin T, Takano H, Dong JH, Haydon PG (2007): Synaptic islands defined by the territory of a single astrocyte. J Neurosci 27:6473–6477.
7. Mulholland PJ, Chandler LJ, Kalivas PW (2016): Signals from the fourth dimension regulate drug relapse. Trends Neurosci 39:472–485.
8. Scofield MD, Heinsbroek JA, Gipson CD, Kupchik YM, Spencer S, Smith AC, *et al.* (2016): The nucleus accumbens: Mechanisms of addiction across drug classes reflect the importance of glutamate homeostasis. Pharmacol Rev 68:816–871.
9. Chaudhry FA, Lehre KP, van Lookeren Campagne M, Ottersen OP, Danbolt NC, Storm-Mathisen J (1995): Glutamate transporters in glial plasma membranes: Highly differentiated localizations revealed by quantitative ultrastructural immunocytochemistry. Neuron 15:711–720.
10. Minelli A, Barbaresi P, Reimer RJ, Edwards RH, Conti F (2001): The glial glutamate transporter GLT-1 is localized both in the vicinity of and at distance from axon terminals in the rat cerebral cortex. Neuroscience 108:51–59.
11. Rusakov DA (2001): The role of perisynaptic glial sheaths in glutamate spillover and extracellular Ca(2+) depletion. Biophys J 81:1947–1959.
12. Pannasch U, Freche D, Dallerac G, Ghezali G, Escartin C, Ezan P, *et al.* (2014): Connexin 30 sets synaptic strength by controlling astroglial synapse invasion. Nat Neurosci 17:549–558.
13. Cheetham JJ, Hilfiker S, Benfenati F, Weber T, Greengard P, Czernik AJ (2001): Identification of synapsin I peptides that insert into lipid membranes. Biochem J 354:57–66.
14. Derouiche A, Frotscher M (2001): Peripheral astrocyte processes: Monitoring by selective immunostaining for the actin-binding ERM proteins. Glia 36:330–341.
15. Lavialle M, Aumann G, Anlauf E, Prols F, Arpin M, Derouiche A (2011): Structural plasticity of perisynaptic astrocyte processes involves ezrin and metabotropic glutamate receptors. Proc Natl Acad Sci U S A 108:12915–12919.
16. Bushong EA, Martone ME, Jones YZ, Ellisman MH (2002): Protoplasmic astrocytes in CA1 stratum radiatum occupy separate anatomical domains. J Neurosci 22:183–192.
17. Reichenbach A, Derouiche A, Kirchhoff F (2010): Morphology and dynamics of perisynaptic glia. Brain Res Rev 63:11–25.
18. Stelzer EHK (1990): The intermediate optical system of laser-scanning confocal microscopes. In: Pawley JB, editor. Handbook of Biological Confocal Microscopy, 3rd ed. New York: Plenum Press, 93–103.
19. Octeau JC, Chai H, Jiang R, Bonanno SL, Martin KC, Khakh BS (2018): An optical neuron-astrocyte proximity assay at synaptic distance scales. Neuron 98:49–66.e49.
20. Scofield MD, Li H, Siemsen BM, Healey KL, Tran PK, Woronoff N, *et al.* (2016): Cocaine self-administration and extinction leads to reduced glial fibrillary acidic protein expression and morphometric features of astrocytes in the nucleus accumbens core. Biol Psychiatry 80:207–215.
21. Kawaguchi K, Yoshida S, Hatano R, Asano S (2017): Pathophysiological roles of ezrin/radixin/moesin proteins. Biol Pharm Bull 40:381–390.
22. Geiger KD, Stoldt P, Schlote W, Derouiche A (2000): Ezrin immunoreactivity is associated with increasing malignancy of astrocytic tumors but is absent in oligodendrogliomas. Am J Pathol 157:1785–1793.
23. Kirik OV, Korzhevskiy DE (2013): Extraependymal ependymocytes in the rat brain [in Russian]. Morfologiia 143:71–73.
24. Zhang Y, Chen K, Sloan SA, Bennett ML, Scholze AR, O'Keeffe S, *et al.* (2014): An RNA-sequencing transcriptome and splicing database of glia, neurons, and vascular cells of the cerebral cortex. J Neurosci 34:11929–11947.
25. Tsukita S, Yonemura S (1999): Cortical actin organization: Lessons from ERM (ezrin/radixin/moesin) proteins. J Biol Chem 274:34507–34510.
26. Reissner KJ, Sartor GC, Vazey EM, Dunn TE, Aston-Jones G, Kalivas PW (2012): Use of vivo-morpholinos for control of protein expression in the adult rat brain. J Neurosci Methods 203:354–360.
27. Testen A, Sepulveda-Orengo MT, Gaines CH, Reissner KJ (2018): Region-specific reductions in morphometric properties and synaptic colocalization of astrocytes following cocaine self-administration and extinction. Front Cell Neurosci 12:246.
28. Robertson JM (2018): The gliocentric brain. Int J Mol Sci 19.
29. Durkee CA, Araque A (2019): Diversity and specificity of astrocyte-neuron communication. Neuroscience 396:73–78.
30. Allen NJ (2014): Astrocyte regulation of synaptic behavior. Annu Rev Cell Dev Biol 30:439–463.
31. Oliveira JF, Sardinha VM, Guerra-Gomes S, Araque A, Sousa N (2015): Do stars govern our actions? Astrocyte involvement in rodent behavior. Trends Neurosci 38:535–549.
32. Shen HW, Scofield MD, Boger H, Hensley M, Kalivas PW (2014): Synaptic glutamate spillover due to impaired glutamate uptake mediates heroin relapse. J Neurosci 34:5649–5657.
33. Henneberger C, Bard L, Panatier A, Reynolds JP, Medvedev NI, Minge D, *et al.* (2019): LTP induction drives remodeling of astroglia to boost glutamate escape from synapses [published online ahead of print Jan 5]. bioRxiv.
34. Danbolt NC (2001): Glutamate uptake. Prog Neurobiol 65:1–105.
35. Dietrich D, Kral T, Clusmann H, Friedl M, Schramm J (2002): Presynaptic group II metabotropic glutamate receptors reduce stimulated and spontaneous transmitter release in human dentate gyrus. Neuropharmacology 42:297–305.
36. Scofield MD, Boger HA, Smith RJ, Li H, Haydon PG, Kalivas PW (2015): Gq-DREADD selectively initiates glial glutamate release and inhibits cue-induced cocaine seeking. Biol Psychiatry 78:441–451.
37. Lehre KP, Rusakov DA (2002): Asymmetry of glia near central synapses favors presynaptically directed glutamate escape. Biophys J 83:125–134.
38. Ventura R, Harris KM (1999): Three-dimensional relationships between hippocampal synapses and astrocytes. J Neurosci 19:6897–6906.
39. Witcher MR, Kirov SA, Harris KM (2007): Plasticity of perisynaptic astroglia during synaptogenesis in the mature rat hippocampus. Glia 55:13–23.
40. Gipson CD, Kupchik YM, Shen H, Reissner KJ, Thomas CA, Kalivas PW (2013): Relapse induced by cues predicting cocaine depends on rapid, transient synaptic potentiation. Neuron 77:867–872.
41. Gipson CD, Kupchik YM, Kalivas PW (2014): Rapid, transient synaptic plasticity in addiction. Neuropharmacology 76(Pt B):276–286.
42. Soares-Cunha C, Coimbra B, Sousa N, Rodrigues AJ (2016): Reappraising striatal D1- and D2-neurons in reward and aversion. Neurosci Biobehav Rev 68:370–386.
43. Lobo MK, Nestler EJ (2011): The striatal balancing act in drug addiction: Distinct roles of direct and indirect pathway medium spiny neurons. Front Neuroanat 5:41.
44. Heinsbroek JA, Neuhofer DN, Griffin WC 3rd, Siegel GS, Bobadilla AC, Kupchik YM, *et al.* (2017): Loss of plasticity in the D2-accumbens pallidal pathway promotes cocaine seeking. J Neurosci 37:757–767.
45. Bobadilla AC, Heinsbroek JA, Gipson CD, Griffin WC, Fowler CD, Kenny PJ, *et al.* (2017): Corticostriatal plasticity, neuronal ensembles, and regulation of drug-seeking behavior. Prog Brain Res 235:93–112.
46. Martin R, Bajo-Graneras R, Moratalla R, Perea G, Araque A (2015): Circuit-specific signaling in astrocyte-neuron networks in basal ganglia pathways. Science 349:730–734.